

Bubble Meets Droplet: Particle-Assisted Reconfiguration of Wetting Morphologies in Colloidal Multiphase Systems

Yi Zhang, Abiola Shitta, J. Carson Meredith,* and Sven H. Behrens*

Wetting phenomena are ubiquitous in nature and play key functions in various industrial processes and products. When a gas bubble encounters an oil droplet in an aqueous medium, it can experience either partial wetting or complete engulfment by the oil. Each of these morphologies can have practical benefits, and controlling the morphology is desirable for applications ranging from particle synthesis to oil recovery and gas flotation. It is known that the wetting of two fluids within a fluid medium depends on the balance of interfacial tensions and can thus be modified with surfactant additives. It is reported that colloidal particles, too, can be used to promote both wetting and dewetting in multifluid systems. This study demonstrates the surfactant-free tuning and dynamic reconfiguration of bubble-droplet morphologies with the help of cellulosic particles. It further shows that the effect can be attributed to particle adsorption at the fluid interfaces, which can be probed by interfacial tensiometry, making particle-induced transitions in the wetting morphology predictable. Finally, particle adsorption at different rates to air–water and oil–water interfaces can even lead to slow, reentrant wetting behavior not familiar from particle-free systems.

1. Introduction

Wetting phenomena are ubiquitous both in nature and in various industrial processes and products.^[1–3] When a liquid droplet is put in contact with a flat homogenous solid surface, three distinct wetting configurations may be found: complete wetting, partial wetting, and non-wetting.^[3] While the wetting of a solid surface has been intensively studied,^[1–3] the wetting morphologies resulting from the encounter of two immiscible fluid droplets within a fluid medium have received less attention. Nevertheless, wetting in disperse multiphase systems plays a major role

in many industrial processes, related e.g., to encapsulation, enhanced oil recovery, water purification, food technology, or defoaming.^[4–15] An analysis of wetting in these systems was first reported in the early 1970s by Torza and Mason^[4] and was revisited recently by Pannacci et al.^[5] and Guzowski et al.^[6] These authors found that the wetting of a liquid droplet by a second fluid in a third immiscible fluid medium can result in three possible wetting morphologies (non-wetting, partial engulfment, and complete engulfment of one drop by the other), which were successfully predicted based on the spreading coefficients of three fluids. A fluid i will spread spontaneously at the interface of two immiscible fluids j and k if its spreading coefficient $S_i = \gamma_{jk} - (\gamma_{ik} + \gamma_{ij})$ is positive, where γ_{ij} , γ_{ik} , and γ_{jk} are the respective interfacial tensions.^[4–6] For the wetting behavior of a colloidal multiphase system, three cases can be distinguished: if the spreading coefficient of the continuous medium phase is positive, the droplets will be non-wetting and try to separate; if, by contrast, one of the droplet phases has a positive spreading coefficient, it will fully engulf the other droplet (complete wetting); the case

Y. Zhang, Dr. A. Shitta, Prof. J. C. Meredith,
Prof. S. H. Behrens
School of Chemical & Biomolecular Engineering
Georgia Institute of Technology
Atlanta, GA 30332-0100, USA
E-mail: carson.meredith@chbe.gatech.edu;
sven.behrens@chbe.gatech.edu



DOI: 10.1002/sml.201600799

of partial wetting is realized when none of the three phases has a positive spreading coefficient.^[4–8] Each of the three wetting configurations has different applications. The complete engulfment of one drop inside another can be used to encapsulate active substances in the inner droplet for controlled release, and has been exploited in contrast-enhanced ultrasonography, gas flotation, encapsulation, and defoaming.^[7,9–11] Partial engulfment is used in the synthesis of anisotropic particles with promise for applications such as drug delivery, imaging, and sensing.^[12] The non-wetting configuration can be used to provide a fluid spacer phase that prevents the coalescence of neighboring plugs in plug-flow microfluidics.^[13] All of these applications call for a specific wetting morphology. A given fluid system, however, does not always adopt the desired wetting configuration; hence there is significant and widespread interest in methods to tune or even actively reconfigure the wetting configuration on demand. Surfactants are the traditional tool for achieving a desired wetting configuration, because they can alter spreading coefficients by adsorbing at fluid–fluid interfaces and reducing their interfacial tensions.^[14] A recent study demonstrates the use of surfactants to actively reconfigure wetting states in a colloidal system consisting of three- and four-phase complex emulsions.^[15]

Unlike surfactants, which adsorb at and desorb from an interface readily as an effect of thermal fluctuations,^[16] particles with suitable wettability can be strongly adsorbed to the interface of immiscible fluids because of high adsorption energy.^[17] Since the pioneering work of Ramsden and Pickering in the early 20th century,^[18] numerous studies have reported the fabrication of ultrastable colloidal multiphase systems, such as foams,^[19] emulsions,^[20] liquid marbles,^[21] colloidosomes,^[22] and bijels,^[23] using colloidal particles. Particle-stabilized colloidal multiphase systems have applications in cosmetics, food products, wastewater treatment, and oil recovery processes. Goedel found that particles can assist the spreading of trimethylpropane trimethacrylate (TMPTMA) at a planar air–water interface.^[24] Although it was recognized more than a century ago that particles can act as stabilizers in colloidal multiphase systems, it is still unknown whether particles can also act as wetting modifiers. For example, can particles be used to induce or prevent the wetting of an oil droplet around gas bubbles in a colloidal multiphase system? One may also wonder whether the wetting configuration in systems with particle-laden interfaces can be predicted based on an effective interfacial tension or spreading coefficient of the particle-coated interface. Another question is whether particles afford the ability to actively reconfigure the wetting morphology, i.e., to change an existing configuration in situ through the controlled addition of appropriately selected particles.

We address these questions in the present paper and demonstrate that the wetting configuration of a colloidal multiphase system can be tuned by selection of appropriate colloidal particles, as predicted by an effective spreading coefficient. The wetting and engulfment of an air bubble by an oil droplet in a water medium was used as a model system because it is relevant in a wide variety of industrial processes such as contrast-enhanced ultrasonography, gas flotation,

and defoaming.^[7,9–11] We also demonstrate that particles can be used both to promote “bubble wetting” and induce the complete bubble engulfment by an oil drop, or to trigger progressive “bubble dewetting”, i.e., to substantially reduce the oil–bubble contact area. A mechanistic understanding of this reconfiguration process was obtained by measuring the effective dynamic surface and interfacial tensions obtained via axisymmetric drop shape analysis. The tunability is attributed to changes in interfacial energy caused by the adsorption of particles at fluid–fluid interfaces. This study yields a new strategy to predict and control the wetting configuration in colloidal multiphase systems, with potential benefits in a wide range of research fields, industrial processes, and commercial products.

2. Results

2.1. Selection of Colloidal Multiphase Systems

Our study focuses on the wetting of an air bubble by an oil droplet in a water medium. We chose hexadecane and tripropylene glycol diacrylate (TPGDA) as oil phases, because these are commonly found in industrial processes and have different wetting in the absence of particles.^[25] Particles of ethyl cellulose (EC) and hydroxypropyl methylcellulose phthalate (hypromellose phthalate, HP 55) were used as wetting modifiers because they are readily available, chemically modifiable, and biorenewable.^[26,27] The hydrodynamic diameters of the EC and HP 55 particles as obtained by dynamic light scattering are 102.3 and 137.4 nm, respectively. The corresponding coefficients of variation are 13% and 10%, respectively. A glass capillary tube with square cross-section was used to observe the wetting configurations of air–water–oil particle combinations. One air bubble and one oil droplet were dispensed from microsyringes, transferred to a square capillary containing the aqueous particle dispersion, and kept stationary for 30 min to allow for particles to adsorb on their surfaces. Then the bubble and oil droplet were brought into contact by slightly tilting the capillary and exploiting the bubble’s buoyancy (see movie S1 in the Supporting Information). The wetting configuration assumed upon bubble–droplet contact was examined optically in the glass capillary.

For a three-phase system, the final wetting morphology can be determined by knowing at least two spreading coefficients.^[4–6] In the scenario of interest to our study, the wetting of an air bubble by an oil drop in an aqueous medium, there are only two kinds of possible wetting configurations: partial and complete wetting. The non-wetting state is energetically unfavorable: because of the high air–water surface tension, γ_{aw} , water cannot spread at an air–oil interface ($S_w = \gamma_{ao} - (\gamma_{aw} + \gamma_{ow}) < 0$ always). Similarly, it is energetically unfavorable for the gas bubble to engulf the oil droplet ($S_a < 0$). Therefore, the final wetting morphology can be determined from knowledge of only the oil spreading coefficient. If the oil phase has a positive spreading coefficient ($S_o > 0$), the oil will engulf the bubble completely, otherwise partial wetting will occur (**Figure 1**).

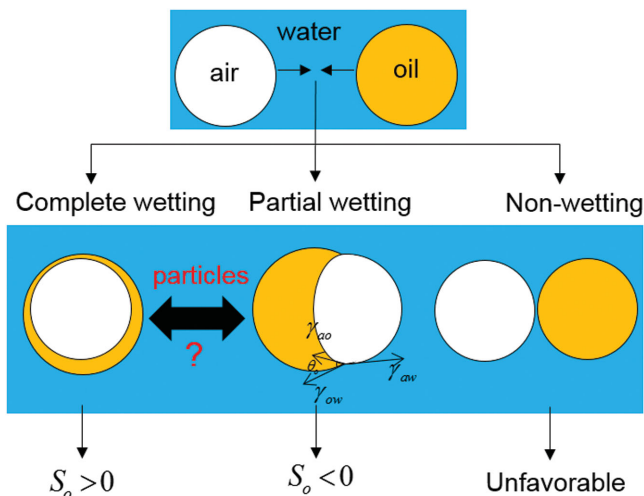


Figure 1. Possible wetting morphologies of an air bubble and an oil droplet in water and schematic illustration of the equilibrium contact angle at the three-phase contact line. Here $S_o = \gamma_{aw} - (\gamma_{ao} + \gamma_{ow})$, where a, o, w denote the air, oil, and water phase, respectively.

2.2. Particles Can Promote Bubble Wetting

Figure 2 shows that the dispersions particle present in the aqueous medium determine the wetting configuration of

the air–hexadecane–water system. In the absence of particles partial engulfment of the bubble by hexadecane was observed (Figure 2a), and the presence of up to 0.2 wt% of EC particles did not change this qualitative behavior (Figure 2b). By contrast, when the air bubble and hexadecane droplet were brought into contact in water containing 0.2 wt% of HP 55 particles, we observed complete bubble engulfment (Figure 2c). We found that these wetting configurations do not change in the following 12 h. These results show that the wetting morphology of air–hexadecane–water system was changed from partial to complete wetting by using as little as 0.2 wt% HP 55 particles.

2.3. The Change in Wetting Morphology Is Attributed to an Interfacial Energy Change Caused by Particle Adsorption

We propose that the dependence of the wetting configuration on the presence and type of particles may be attributed to the tuning of interfacial tensions caused by the adsorption of particles in the interfaces.^[28] We employed dynamic surface tension measurements, which have proven to be a straightforward and powerful method of quantifying the effective surface or interfacial tension of fluid interfaces containing adsorbed particles.^[28,29] The measured effective surface and interfacial tension data yield an effective spreading coefficient of fluid *i* via

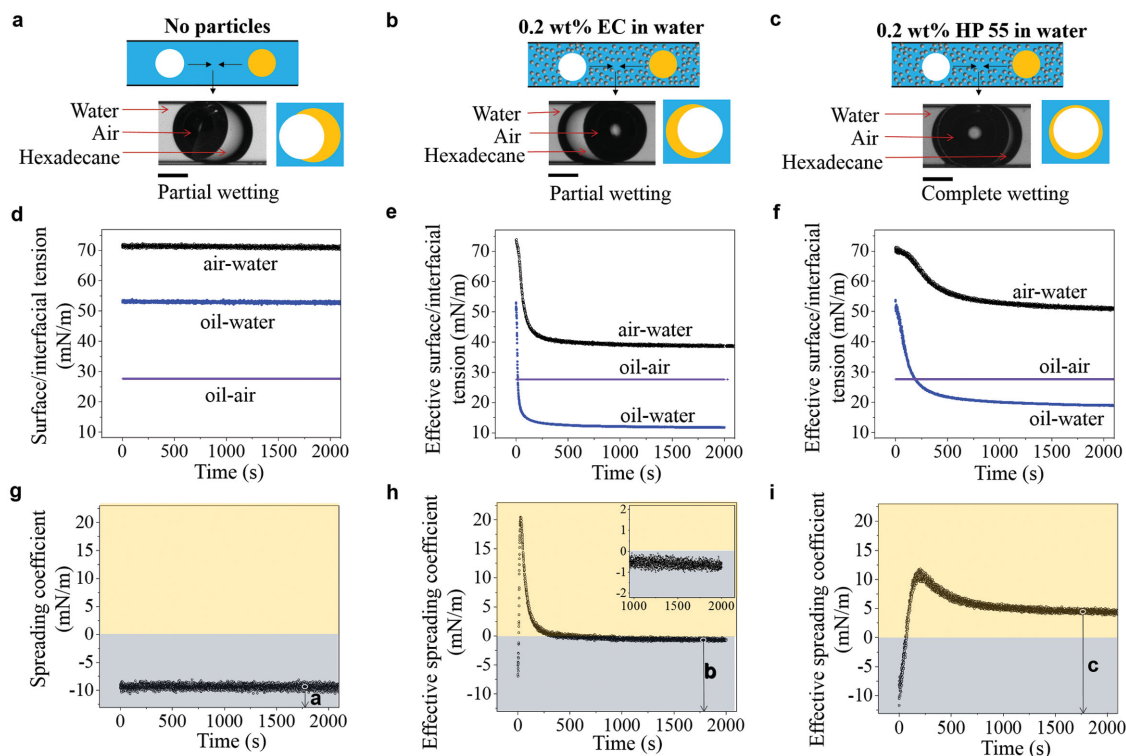


Figure 2. Particles can promote bubble wetting. First row: experimental observations of an air bubble and a hexadecane droplet brought into contact in a water medium containing a) no particles, b) 0.2 wt% EC particles, and c) 0.2 wt% HP 55 particles. Scale bars are 500 μm . Second row: the dynamic effective surface and interfacial tension of an air–hexadecane–water system in which the water phase contains d) no particles, e) 0.2 wt% EC particles, and f) 0.2 wt% HP 55 particles. Third row: the dynamic effective spreading coefficient of an air–hexadecane–water system in which the water phase contains g) no particles, h) 0.2 wt% EC particles, and i) 0.2 wt% HP55 particles. The yellow band indicates the complete wetting regime as predicted based on the positive effective spreading coefficient ($S'_o > 0$), the gray band indicates the partial wetting regime expected for a negative effective spreading coefficient ($S'_o < 0$).

$$S'_i = \gamma'_{jk} - (\gamma'_{ij} + \gamma'_{ik}) \quad (1)$$

We measured the interfacial tension via analysis of a pendant drop shape, which is determined by a balance of gravitational and tension forces.^[28,29] Figure 2d–f show time-dependent drop shape tensiometry measurements for the air–water and hexadecane–water interfaces, in which the water phase contained no particles, 0.2 wt% EC particles, or 0.2 wt% HP 55 particles, respectively. When the water phase contained no particles, the tension of the air–water interface and of the hexadecane–water interface were time independent (Figure 2d). On the other hand, when the water phase contained 0.2 wt% HP 55 or 0.2 wt% EC particles, the effective air–water tension γ'_{aw} and effective hexadecane–water tension γ'_{ow} first decreased with time and then reached steady state (Figure 2e,f). The decrease in γ'_{aw} and γ'_{ow} is caused by the progressive adsorption of particles at the respective interface over the course of the measurement series.^[28,29] As the interface reaches a plateau coverage by particles, the effective surface and interfacial tension also reached steady value.^[28,29] The particles may also adsorb on the oil–air interface when an air bubble and an oil droplet are brought into contact. In principle the adsorption of particles at the oil–air interface can also influence the tension of the oil–air interface. Contact angle experiments however suggest that the particles have little influence on the effective oil–air surface tension; they are shown in the Supporting Information. We therefore make the simplifying assumption of a constant effective tension at the air–hexadecane interface. Using Equation (1), we obtained the effective dynamic spreading coefficient of hexadecane (shown in Figure 2g–i). In our experiment, the air bubble and hexadecane droplet were retained in the water phase for around 30 min to allow particles to adsorb to the interfaces. Therefore, the values of the effective spreading coefficient at 30 min were used. Figure 2g shows that the oil spreading coefficient in the absence of particles is negative in agreement with the observed partial bubble engulfment. The presence of 0.2 wt% EC particles in the water phase raises the effective spreading coefficient significantly by reducing the oil–water interfacial tension (Figure 2e), but the effect on the spreading coefficient is partly offset by a significant simultaneous reduction of the air–water tension, which results in a negative value of $S'_o = -0.7 \text{ mN m}^{-1}$ after 30 min (Figure 2h). The presence of 0.2% HP 55 particles, by contrast, reduces the oil–water tension much more than it does the air–water tension (Figure 2f), and therefore leads to positive values of the effective spreading coefficient S'_o after 3 min (Figure 2i). As mentioned before, a positive effective spreading coefficient is consistent with the complete bubble engulfment by the oil droplet, whereas a negative value indicates only partial engulfment. The predicted morphologies based on the effective spreading coefficient matched the directly observed wetting configurations in a water phase containing no particles, 0.2 wt% EC particles, and 0.2 wt% HP 55 particles, respectively. For the wetting of air–hexadecane–water in the presence of 0.2 wt% EC particles, the accuracy of the wetting prediction based on the measured effective spreading coefficient may appear doubtful, because the experimental value is very close to the threshold value of zero (within

the estimated uncertainty of the tension measurements on the order of 1 mN m^{-1}). Visual observation and tensiometry, however, consistently suggest that partial wetting occurs. Additionally, we observed that a hexadecane droplet placed on the macroscopic surface of an aqueous 0.2 wt% EC particle dispersion formed a stable oil lens with a finite contact angle rather than a wetting film (Figure S9, Supporting Information). It therefore seems safe to conclude that in the particle dispersion the steady-state wetting configuration of an air bubble and a hexadecane droplet is indeed one of partial bubble engulfment.

2.4. Particles Can Promote Bubble Dewetting

As the observations of Figure 2 demonstrate, particles can promote bubble wetting and induce the complete bubble engulfment by hexadecane. One may wonder whether particles can also be used to promote bubble dewetting and reduce the wetting area between an oil droplet and a gas bubble. To answer this question, we turned to a system in which hexadecane was replaced by the more polar TPGDA. Since TPGDA has a non-negligible water solubility of 4 g L^{-1} , we mutually saturated the TPGDA and water phase before performing the experiments and interfacial measurements so that equilibrium was reached. In the absence of particles, this system experiences partial engulfment of the air bubble by the oil as seen in **Figure 3a**. Although the systems maintain partial wetting in the presence of 0.2 wt% EC or HP 55 particles in the water phase (Figure 3b, c), the presence of 0.2 wt% EC particles in the water phase induces further dewetting and substantially reduces the oil–bubble contact (Figure 3b). It can be quantified by the equilibrium contact angle at the three-phase contact line (Figure 1).^[6] For the contact angle θ_o , measured through oil phase,

$$\cos \theta_o = \frac{\gamma'_{aw}{}^2 - (\gamma'_{ow}{}^2 + \gamma'_{ao}{}^2)}{2\gamma'_{ow}\gamma'_{ao}} \quad (2)$$

where γ'_{aw} , γ'_{ao} , and γ'_{ow} are the respective interfacial tensions and a, w, o denotes air, water, oil phase, respectively. By analyzing the dynamic surface and interfacial tensions (shown in Figure 3d,e), we found that the effective spreading coefficient of TPGDA changes from -2.4 mN m^{-1} without particles to -7.8 mN m^{-1} in the presence of 0.2 wt% EC particles. The corresponding three-phase contact angle measured through the oil phase increased from 43.2° to 87.4° . These results suggest that particles can be used to promote “bubble dewetting” and substantially reduce the oil–bubble contact area. We also note in passing that if the experiment is carried out with unsaturated TPGDA and water phases, the initial oil spreading coefficient is positive and the bubble gets fully engulfed by the oil. In the absence of particles, a slow transition to partial engulfment over several hours can then be observed as partial mixing of the liquids in the interfacial region proceeds and shifts the balance of interfacial tensions toward a negative oil spreading coefficient (Figure S4a,b, Supporting Information). In the presence of 0.2 wt% EC particles, by contrast, the transition from complete to partial

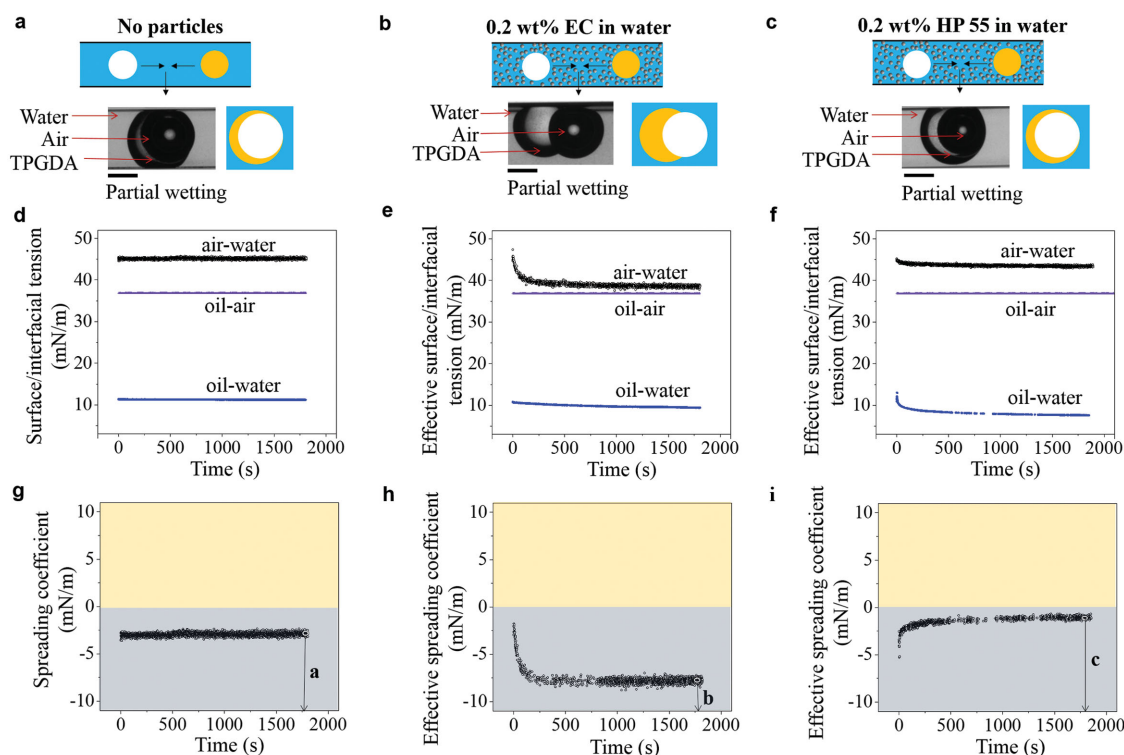


Figure 3. Particles can promote bubble dewetting. Experimental observations of an air bubble and a TPGDA droplet brought into contact in a water phase containing a) no particles, b) 0.2 wt% EC particles, and c) 0.2 wt% HP 55 particles. Scale bars are 500 μm . The dynamic effective surface and interfacial tension of an air–TPGDA–water system in which the water phase contains d) no particles, e) 0.2 wt% EC particles, and f) 0.2 wt% HP 55 particles. The dynamic effective spreading coefficient of an air–TPGDA–water system in which the water phase contains g) no particles, h) 0.2 wt% EC particles, and i) 0.2 wt% HP55 particles. The yellow and gray background indicate the different wetting regimes as in Figure 2.

engulfment happens in less than 10 min (Figures S4c,d), and eventually the system reaches the same final state depicted in Figure 3b.

2.5. Wetting Behavior as Function of Particle Concentration

In Figures 2 and 3, only one specific particle concentration (0.2 wt%) was used to demonstrate that particles can be used to change the wetting configurations. We have further investigated the effect of particle concentration (Figure 4). Figure 4a shows the stable wetting morphologies and the corresponding effective spreading coefficients of the air–hexadecane–water system for different concentrations of the HP 55 particles (from experiments analogous to those shown in Figure 2c,f,i). Both the visual observation of the bubble–droplet pairs and measured effective spreading coefficient suggest that the wetting morphology changes from partial to complete wetting at the particle concentration around 0.02 wt%. Figure 4b shows the corresponding wetting morphologies and effective spreading coefficients of the air–TPGDA–water system in the presence of various concentrations of EC particles (experiments analogous to those shown in Figure 3b,e,h). The observed wetting configuration demonstrates that the presence of only 0.01 wt% already gives rise to significant bubble dewetting, whereas the measured effective spreading coefficient suggests that the effect plateaus at a somewhat higher concentration (around 0.03 wt%).

This difference might be explained by the difficulty of comparing droplet images taken at slightly different viewing angles and the possibility that full equilibrium had not been reached within the experimental observation period at these very low particle concentrations.

2.6. Direct Observation of the Interfacially Adsorbed Particles

The hypothesis that particle adsorption at the fluid–fluid interfaces is indeed the cause for the observed modulation of the wetting configurations was further supported by confocal microscopy. The EC and HP 55 particles were labeled with Nile red. When the air bubble and hexadecane droplet were brought into contact in water containing 0.2 wt% Nile red labeled-HP 55 particles, we observed complete bubble engulfment (Figure 5a), the same wetting configuration found in the presence of label-free HP 55 particles. The confocal micrograph and the intensity profile (Figure 5d) indicate an accumulation of the HP 55 particles at the hexadecane–water interface. This particle adsorption reduces the energetic penalty (tension) of the oil–water interface, thus promoting its expansion. When the air bubble and hexadecane droplet were brought into contact in water containing Nile red labeled EC particles, we observed that the system retained the partial bubble engulfment, even when the particle concentration was doubled to 0.4 wt% (Figure 5b,c). Confocal images and the fluorescence intensity profiles

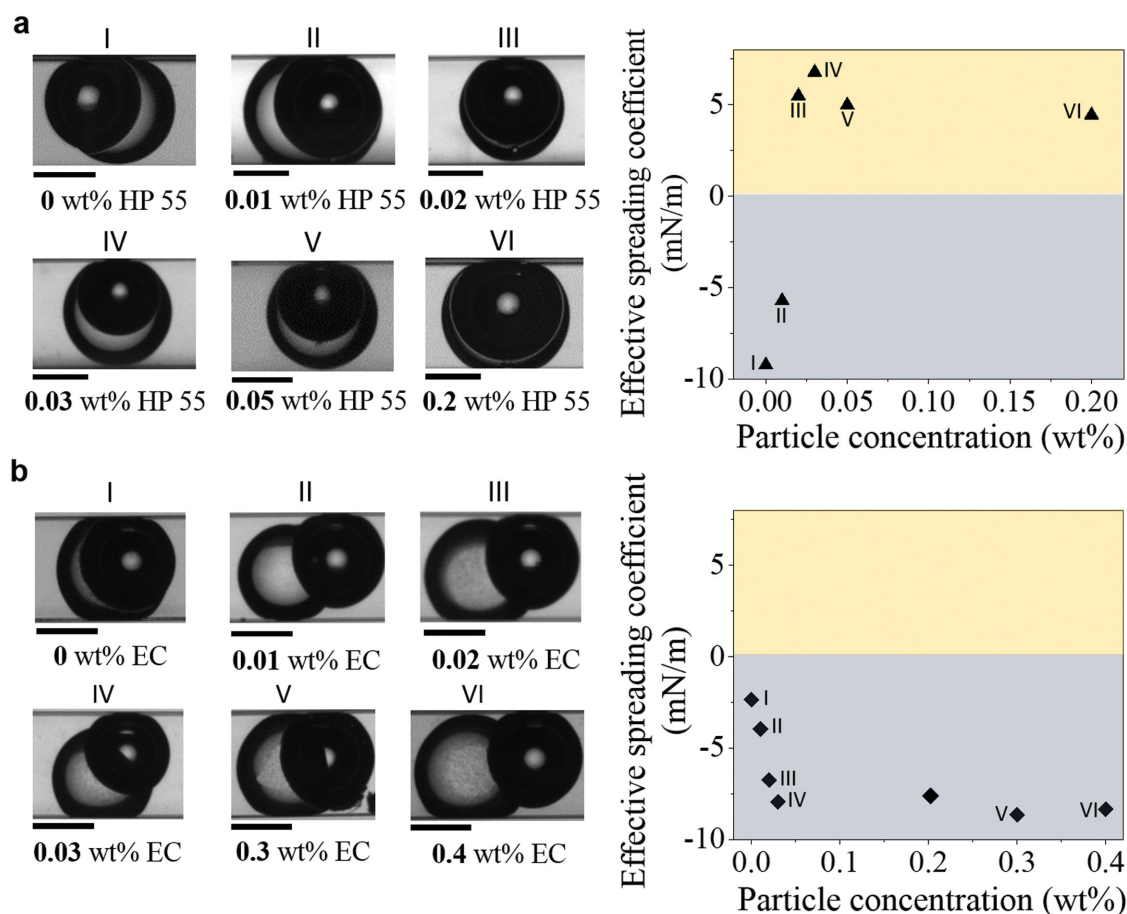


Figure 4. Wetting behavior as a function of particle concentration. a) Wetting morphologies and corresponding effective oil spreading coefficients for the air-hexadecane-water system at different concentrations of hypromellose phthalate particles (HP 55). b) Wetting morphologies and corresponding effective oil spreading coefficients for the air-TPGDA-water system at different concentrations of ethyl cellulose (EC) particles. Scale bars are 500 μm .

suggest that EC particles accumulate at both the air-water and hexadecane-water interface (Figure 5b,c,e,f). Again, the particle adsorption in the hexadecane-water interface reduces the effective oil-water interfacial tension and raises the oil spreading coefficient, but in the case of EC particles the competing adsorption in the air-water interface (Figure 5b,e) is also strong and mitigates the increase in the oil spreading coefficient, keeping its final value below zero (Figure 2h). We note that the fluorescence intensity from particles at the air-water interface (Figure 5e) in fact exceeds the intensity recorded from the oil-water interface (Figure 5f), for which the particle-induced reduction of interfacial tension is nonetheless more pronounced (Figure 2e,h). To appreciate why these observations are not inconsistent, we point out that the fluorescence intensity does not lend itself for direct comparison of the particle concentrations in the two interfaces, because it also depends on the fluid environment, while that the reduction in interfacial tension depends not only on the interfacial particle concentration, but also on the particle contact angle with the interface (for details see section 8 of the Supporting Information).

2.7. In Situ Reconfiguration of Pre-established Wetting Morphologies

In addition to tuning the wetting configuration through the selection of particles, we also studied the dynamic, in situ change of pre-formed wetting morphologies upon addition of particles to the system. An air bubble and an oil droplet, both suspended in the water phase, were brought into contact in a glass tube open at both ends. This tube was then placed into a particle dispersion containing either 0.4 wt% EC or 0.2 wt% HP 55 particles (Figure 6a). As HP 55 particles diffused into the tube, we observed that the wetting morphology changed from partial to complete wetting for the air-hexadecane-water three-phase system over the course of 15 min (Figure 6b, Figure S6a, Supporting Information). A substantial reduction of oil-bubble contact area was seen when exposing the air-TPGDA-water three-phase system to the EC particle dispersion (Figure 6c). The final configurations observed here match the ones seen when the particles are present before the bubble and oil droplet are brought into contact (Figures 2 and 3). The experiments of Figure 6 show that the particles can be used to reconfigure

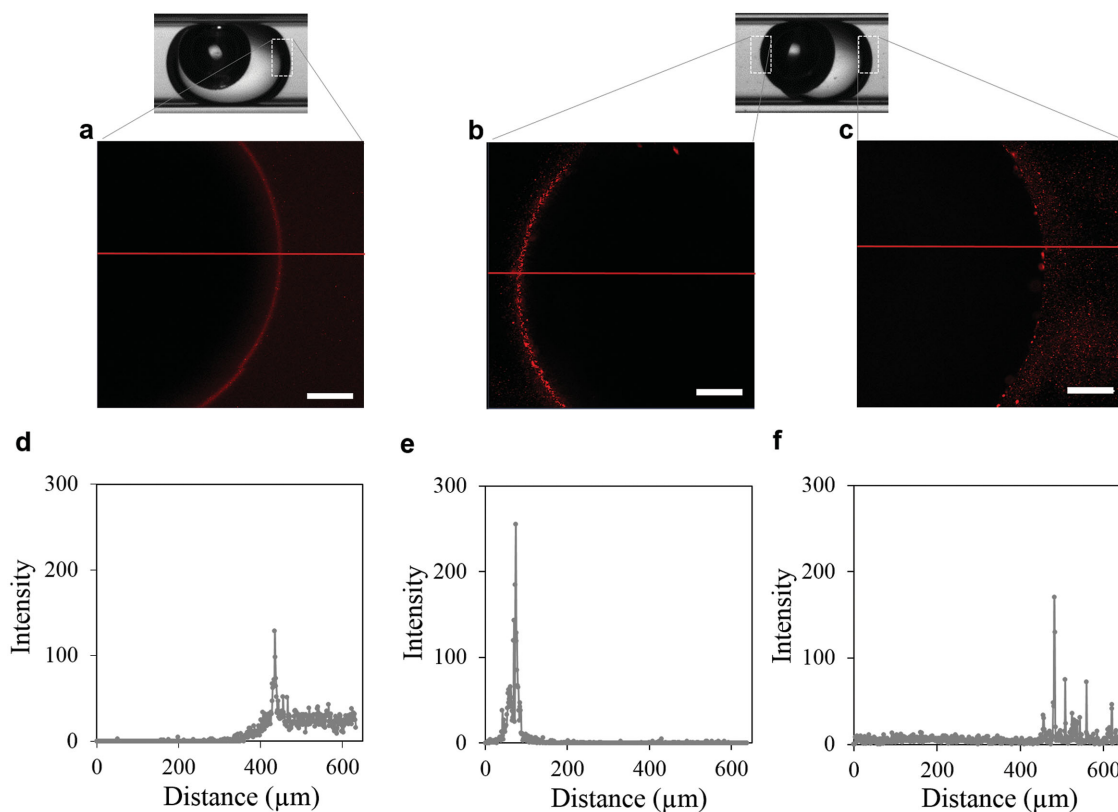


Figure 5. Visualization of interfacially adsorbed particles that affect the wetting configuration. a) Confocal microscope images of a close-up of the hexadecane–water interface when an air bubble and a hexadecane droplet were brought into contact in a water medium containing 0.2 wt% Nile red labeled HP 55 particles. Confocal microscope images of a close-up of b) the air–water interface and c) the hexadecane–water interface when an air bubble and a hexadecane droplet were brought into contact in a water medium containing 0.4 wt% Nile red labeled EC particles. Scale bars are 100 μm. d–f) The fluorescence intensity profiles along a line across the confocal images in parts a, b, and c, respectively.

an already established wetting state in situ. We expect that this novel capability of dynamically tuning the wetting morphology in colloidal multi-phase systems with particles will provide new impulses for the development of advanced materials.

2.8. Particle-Induced Reentrant Wetting Behavior

We have demonstrated that particles can be used as wetting modifiers (Figures 2, 3, 4, and 6). Figure 2b indicated that the presence of 0.2 wt% of EC particles did not qualitatively change the equilibrium wetting behavior of air–hexadecane–water system, but dynamic interfacial tensiometry (Figure 2e) suggested an effective spreading coefficient (Figure 2h) that transiently assumes positive values before dropping back below zero. This suggests that particles may induce a reentrant wetting behavior, with a transition from partial to complete and back to partial bubble engulfment by the oil, and such behavior was indeed observed. To test whether this reentrant wetting can also be observed upon exposure of a pre-established, partially engulfed bubble to the particles, we carried out a dynamic reconfiguration experiment analogous to those described by Figure 6: An open glass tube, filled with an air bubble partially engulfed by hexadecane

in particle-free water and held horizontally, was placed into a particle dispersion containing 0.2 wt% EC particles. As the particles diffused into the tube, we observed that the wetting morphology changed from partial to complete bubble engulfment within the first 2 min (Figure 7), and then back to partial engulfment over the course of 3 h. To our knowledge, such slow and reentrant bubble or droplet wetting has never been observed in particle-free systems (with surfactants as wetting modifiers).

Both the tension of the air–water interface and of the hexadecane–water interface decrease with time as a result of interfacial particle adsorption (Figure 2e, and a close-up of the initial change in Figure S10c, Supporting Information). As the figure shows, the rate of tension reduction is larger for the oil–water interface than for the air–water interface, which can be attributed to the faster rate of particle adsorption to the oil–water interface. It is well known that both bare oil–water and air–water interfaces tend to carry negative electric surface charge, most likely due to the adsorption of hydroxyl ions.^[30] EC particles in water are also negatively charged (with zeta potential of –50 mV at pH 6). Electric double-layer interaction and image charge repulsion can result in an electrostatic barrier to particle adsorption to the interface,^[31] and one may expect the barrier to be higher at the interface with the larger jump in the dielectric permittivity,

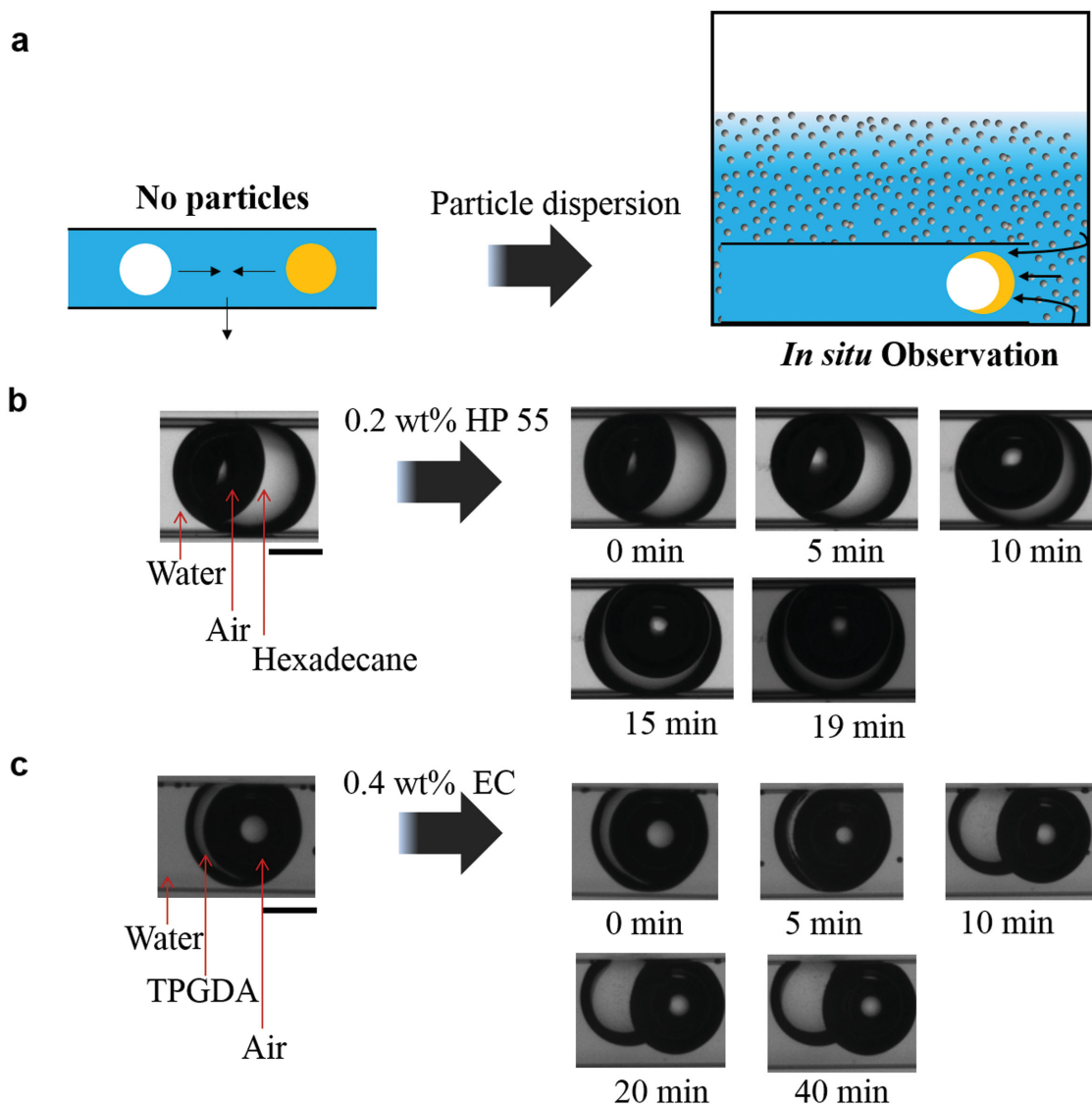


Figure 6. In situ transition of the wetting morphology as particles diffuse to the interfaces. a) Schematic illustration of the experimental procedure: an air bubble and an oil droplet are brought into contact in a particle-free water phase inside an open microfluidic glass channel, which is then placed in a particle suspension containing either 0.2 wt% HP 55 or 0.4 wt% EC particles. b) Wetting morphology transition for the air–hexadecane–water system upon exposure to HP 55 particles. c) Wetting morphology transition for the air–TPGDA–water system upon exposure to EC particles. Scale bars are 500 μm .

i.e., the air–water interface. We therefore speculate that faster particle adsorption to the oil–water interface may result from a weaker adsorption barrier in the oil–water interface. Similar dynamic tension effects were also found for negatively charged silica particles (with a zeta potential of -46.3 mV) adsorbing to air–water and hexadecane–water interfaces (Figure S11 of the Supporting Information). In the reentrant wetting shown in Figure 7, the fast reduction of the effective interfacial tension at the hexadecane–water interface initially causes the effective oil spreading coefficient to become positive and triggers the complete bubble engulfment by the oil (Figure 2h, Figures S10b,d, Supporting Information). Once the air–water interface has been completely replaced by the oil film, a new air–water interface (i.e., a hole in the engulfing oil film) first has to nucleate before that new interface can grow and be stabilized by adsorbing particles. The

exact mechanism for this dewetting transition is unclear—nucleation may, e.g., be facilitated by particle adsorption at the thinnest region of the oil layer—but it seems plausible that this nucleation and growth would take far longer than particle adsorption to a readily available interface. We also note that similar surfactant-induced transitions from complete to partial engulfment^[5] and even the inversion of complete engulfment morphologies^[15] (but no reentrant wetting phenomena) have been reported in recent studies on systems of immiscible liquid droplets.

3. Discussion

In this work, we reported that particles can be used both to promote “bubble wetting” and to trigger “bubble dewetting.”

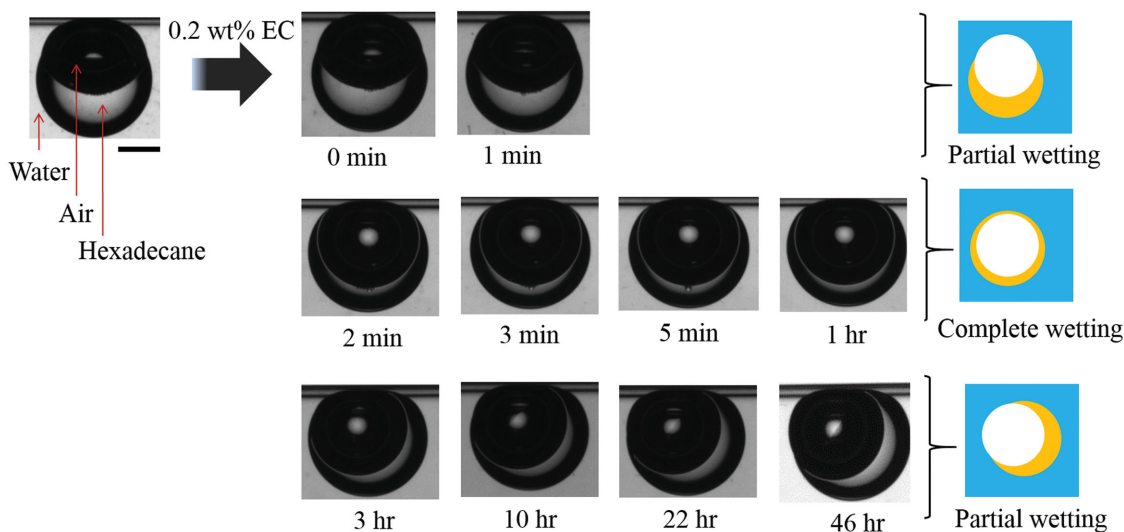


Figure 7. Reentrant wetting transition observed for the air–hexadecane–water system upon exposure to 0.2 wt% EC particles. Particles were introduced as sketched in Figure 6a, the scale bar is 500 μm .

Commercially available EC or HP 55 particles could contain impurities, which tend to be surface-active and may affect the wetting configuration. In order to purify the particle suspension used in the current study and remove any surface-active contaminants, the EC and HP 55 particle suspensions were passed three times through a C18–silica chromatographic column (Phenomenex) that had been preactivated with an acetonitrile–water (80:20) mixture and flushed several times with hot DI water.^[32] In addition, we studied the dynamic surface tensions of supernatants of EC and HP 55 particles after centrifuging their particle dispersions. These surface tension measurements show close agreement with the surface tension of ultrapure DI water (Figures S2a,b, Supporting Information) and suggest that there are no significant surface-active contamination or impurities in the EC and HP 55 particle suspension used in our study. Therefore, we can conclude that the particles themselves, not contaminants, are responsible for the reconfiguration of the wetting morphology.

The central result of our study is that the adsorption of particles at fluid–fluid interfaces provides a novel, surfactant-free method of tuning and reconfiguring wetting morphologies in colloidal multiphase systems. The adsorbed particles can act as not only wetting modifiers but also as efficient stabilizers. Although surfactants can be used to tune interfacial wetting configurations in these systems, there are a number of reasons why particle-based wetting adjustments are interesting. Surfactants are prone to chemical degradation under harsh application conditions and their tendency to fluctuate into and out of the interface can reduce the stability of a wetting configuration.^[33,34] Furthermore, the potential toxicity and environmental accumulation of certain surfactants is problematic for some applications.^[35] Finally, surfactants can be difficult to recover from the final product, which is a significant concern in products requiring high purity or surfactant reuse.^[36] Colloidal particles do not share most of these problems, although their comparatively slow diffusion can sometimes be a disadvantage, and their

size makes it harder to stabilize submicron-sized droplets or bubbles. Hazardous organic surfactants could be avoided and replaced by environmentally friendly, biorenewable, or even food-grade particles in cosmetic, pharmaceutical, or food applications.^[37,38] Furthermore, particles offer convenient options for separation and recovery by filtration or centrifugation. As in the case of most particle-coated emulsion droplets or air bubbles (in Pickering emulsions and foams),^[19,20] the adsorption of particulate wetting modifiers should be practically irreversible because of the high adsorption energy typical for colloidal particles, and lead to the formation of very stable wetting states in the colloidal multiphase system. With this in mind, the demonstrated ability of colloidal particles to dynamically reconfigure wetting configurations, in a way previously known only from the far more mobile and reversibly adsorbing molecular surfactants, appears truly remarkable.

4. Conclusion

We have reported a new strategy for tuning the wetting configuration of colloidal multiphase systems. Through the adsorption of cellulosic particles at fluid–fluid interfaces, a change of surface and interfacial tensions was achieved, as determined by dynamic pendant drop tensiometry. The wetting morphology predicted by the effective spreading coefficient, calculated from dynamic tensiometry data, agrees with the directly observed wetting configurations. In addition, particles can induce slow, reentrant wetting behavior. This study provides a new strategy for controlling and predicting the wetting configuration of an air bubble and an oil droplet in a water medium, which is relevant to a wide variety of materials research problems, industrial processes, and commercial products. We expect the tuning method presented here to be more general and applicable also to other types of particles and colloidal multiphase systems, such as complex emulsions of three or four immiscible liquids.^[5,15] Furthermore,

the tunability of interfacial tensions via particle adsorption suggests that particles can also be useful as wetting modifiers in liquid–liquid–solid and liquid–vapor–solid systems.

5. Experimental Section

A Single Air Bubble and Oil Droplet Were Generated and Brought into Contact: The experimental setup consisted of one square capillary (VitroCom, Inc., with an inner diameter of 1 mm and an outer diameter of 1.4 mm unless otherwise mentioned) to hold the sample and two round capillary tubes (VitroCom, Inc., with an inner diameter of 0.7 mm, an outer diameter of 0.87 mm) through which the air bubble and oil droplet were injected. The square capillary was pretreated with “piranha solution” (a 3:1 mixture of concentrated sulfuric acid and 30% hydrogen peroxide) for 1.5 h. One end of each round capillary tube was shaped into a tapered orifice using a flaming/brown micropipette puller; this end could be used to introduce the air bubble or oil droplet. The other end of the round capillary was connected to a microsyringe (containing air or oil) by using polytetrafluoroethylene (PTFE) tubing. A single air bubble was generated in a petri dish with DI water or particle suspension using a microsyringe and then transferred into the square capillary prefilled with DI water or particle suspension (Figure S3a, Supporting Information). Next, a single oil droplet was dispensed directly into the square capillary through the second injection tube with a slowly and manually operated microsyringe (Figure S3b, Supporting Information). The generated bubble and oil droplet were kept in the device to allow particles to adsorb on the bubble and oil droplet surfaces (Figure S3c, Supporting Information); then they were brought into contact through the buoyancy force on the air bubble (Figure S3d, Supporting Information as seen in movie S1, Supporting Information). The morphologies were studied in the microfluidic device after the air bubble and oil drop made contact (Figure S3e, Supporting Information). The radius of oil droplet and air bubble was always $\approx 300\text{--}400\ \mu\text{m}$.

Measurement of Interfacial Tensions: The dynamic surface and interfacial tension were measured via axisymmetric drop shape analysis of pendant drops with a Ramé-hart goniometer. This method has proven extremely useful to determine the evolution of the interfacial tension due to the adsorption of particles to the interface.^[28,29] Briefly, an inverted pendant drop of oil or an air bubble immersed in the aqueous phase was created by a syringe with a steel needle, and a high speed CCD camera was programmed to capture the variation of drop/bubble shape with time. The interfacial/surface tension is obtained by analyzing the contour shape resulting from the balance of gravitational forces and tension forces. All experiments were performed at room temperature of 21 °C.

Supporting Information

Supporting Information is available from the Wiley Online Library or from the authors.

Acknowledgements

The authors gratefully acknowledge financial support from the National Science Foundation (CBET-1134398), the Air Force Office of Scientific Research (Grant # FA9550-10-1-0555) and fellowship support for Y. Z. by the Renewable Bioproduct Institute (RBI), Georgia Institute of Technology. The authors thank the generous donation of particles from Shin Etsu Chemical Co., Ltd. (Tokyo, Japan). Helpful discussions with Joanna Tsao and Joohyung Lee about the purification of hexadecane and dynamic surface tension measurements are also greatly appreciated.

- [1] D. Myers, *Surfaces, Interfaces, and Colloids: Principles and Applications*, Wiley-VCH, Weinheim, Germany **1991**.
- [2] T. S. Wong, S. H. Kang, S. K. Y. Tang, E. J. Smythe, B. D. Hatton, A. Grinthal, J. Aizenberg, *Nature* **2011**, *477*, 443.
- [3] a) M. J. Liu, Z. X. Xue, H. Liu, L. Jiang, *Angew. Chem. Int. Ed.* **2012**, *51*, 8348; b) Y. Tian, B. Su, L. Jiang, *Adv. Mater.* **2014**, *26*, 6872.
- [4] S. Torza, S. Mason, *J. Colloid Interface Sci.* **1970**, *33*, 67.
- [5] N. Pannacci, H. Bruus, D. Bartolo, I. Etchart, T. Lockhart, Y. Hennequin, H. Willaime, P. Tabeling, *Phys. Rev. Lett.* **2008**, *101*, 164502.1.
- [6] J. Guzowski, P. M. Korczyk, S. Jakiela, P. Garstecki, *Soft Matter* **2012**, *8*, 7269.
- [7] a) J. H. Xu, R. Chen, Y. D. Wang, G. S. Luo, *Lab Chip* **2012**, *12*, 2029; b) L. Yang, K. Wang, S. Mak, Y. K. Li, G. S. Luo, *Lab Chip* **2013**, *13*, 3355; c) J. Rodriguez-Rodriguez, A. Sevilla, C. Martinez-Bazan, J. M. Gordillo, *Annu. Rev. Fluid Mech.* **2015**, *47*, 405.
- [8] a) N. N. Deng, W. Wang, X. J. Ju, R. Xie, D. A. Weitz, L. Y. Chu, *Lab Chip* **2013**, *13*, 4047; b) D. G. Wang, X. P. Huang, Y. P. Wang, *Langmuir* **2014**, *30*, 14460.
- [9] a) R. Moosai, R. A. Dawe, *Sep. Purif. Technol.* **2003**, *33*, 303; b) C. Grattoni, R. Moosai, R. A. Dawe, *Colloids Surf., A* **2003**, *214*, 151; c) M. Eftekhardakhah, G. Øye, *Environ. Sci. Technol.* **2013**, *47*, 14154.
- [10] a) F. Tiarks, K. Landfester, M. Antonietti, *Langmuir* **2001**, *17*, 908; b) L. Y. Chu, A. S. Utada, R. K. Shah, J. W. Kim, D. A. Weitz, *Angew. Chem. Int. Ed.* **2007**, *46*, 8970.
- [11] a) P. R. Garrett, *Defoaming: Theory and Industrial Applications*, Marcel Dekker, New York **1993**; b) N. D. Denkov, K. G. Marinova, S. S. Tcholakova, *Adv. Colloid Interface Sci.* **2014**, *206*, 57.
- [12] a) A. Walthar, A. H. Müller, *Chem. Rev.* **2013**, *113*, 5194; b) S. Lone, I. Cheong, *RSC Adv.* **2014**, *4*, 13322; c) X. P. Huang, Q. P. Qian, Y. P. Wang, *Small* **2014**, *10*, 1412.
- [13] D. L. Chen, L. Li, S. Reyes, D. N. Adamson, R. F. Ismagilov, *Langmuir* **2007**, *23*, 2255.
- [14] D. F. Evans, H. Wennerstrom, *The Colloidal Domain*, Wiley-VCH, Weinheim **2001**.
- [15] L. D. Zarzar, V. Sresht, E. M. Sletten, J. A. Kalow, D. Blankschtein, T. M. Swager, *Nature* **2015**, *518*, 520.
- [16] a) B. P. Binks, *Curr. Opin. Colloid Interface Sci.* **2002**, *7*, 21; b) B. P. Binks, T. S. Horozov, *Colloidal Particles at Liquid Interfaces*, Cambridge University Press, Cambridge **2006**.
- [17] V. Poulichet, V. Garbin, *Proc. Natl. Acad. Sci. USA* **2015**, *112*, 5932.
- [18] a) W. Ramsden, *Proc. R. Soc.* **1903**, *72*, 156; b) S. U. Pickering, *J. Chem. Soc. Trans.* **1907**, *91*, 2001.
- [19] a) R. G. Alargova, D. S. Warhadpande, V. N. Paunov, O. D. Velev, *Langmuir* **2004**, *20*, 10371; b) B. P. Binks, T. S. Horozov, *Angew. Chem. Int. Ed.* **2005**, *44*, 3722; c) U. T. Gonzenbach, A. R. Studart, E. Tervoort, L. J. Gauckler, *Angew. Chem. Int. Ed.* **2006**, *45*, 3526; d) Y. Zhang, J. Wu, H. Wang, J. C. Meredith, S. H. Behrens, *Angew. Chem. Int. Ed.* **2014**, *126*, 13603.

- [20] a) Z. F. Li, T. Ming, J. F. Wang, T. Ngai, *Angew. Chem. Int. Edit.* **2009**, *48*, 8490; b) M. Destribats, S. Gineste, E. Laurichesse, H. Tanner, F. Leal-Calderon, V. Heroguez, V. Schmitt, *Langmuir* **2014**, *30*, 9313.
- [21] a) P. Aussillous, D. Quere, *Nature* **2001**, *411*, 924; b) B. P. Binks, R. Murakami, *Nat. Mater.* **2006**, *5*, 865.
- [22] a) A. D. Dinsmore, M. F. Hsu, M. G. Nikolaides, M. Marquez, A. R. Bausch, D. A. Weitz, *Science* **2002**, *298*, 1006; b) A. S. Miguel, S. H. Behrens, *Soft Matter* **2011**, *7*, 1948.
- [23] E. M. Herzig, K. A. White, A. B. Schofield, W. C. K. Poon, P. S. Clegg, *Nat. Mater.* **2007**, *6*, 966.
- [24] a) H. Xu, W. A. Goedel, *Langmuir* **2003**, *19*, 4950; b) H. Xu, W. A. Goedel, *Angew. Chem. Int. Ed.* **2003**, *42*, 4694; c) A. L. Ding, B. P. Binks, W. A. Goedel, *Langmuir* **2005**, *21*, 1371; d) A. Ding, W. A. Goedel, *J. Am. Chem. Soc.* **2006**, *128*, 4930.
- [25] A. A. Keller, M. J. Chen, *Water Resour. Res.* **2003**, *39*, 1288, DOI:10.1029/2003WR002071.
- [26] a) H. A. Wege, S. Kim, V. N. Paunov, Q. X. Zhong, O. D. Velev, *Langmuir* **2008**, *24*, 9245; b) S. Lam, E. Blanco, S. K. Smoukov, K. P. Velikov, O. D. Velev, *J. Am. Chem. Soc.* **2011**, *133*, 13856; c) E. Blanco, S. Lam, S. K. Smoukov, K. P. Velikov, S. A. Khan, O. D. Velev, *Langmuir* **2013**, *29*, 10019.
- [27] a) H. J. Jin, W. Z. Zhou, J. Cao, S. D. Stoyanov, T. B. J. Blijdenstein, P. W. N. de Groot, L. N. Arnaudov, E. G. Pelan, *Soft Matter* **2012**, *8*, 2194; b) S. Lam, K. P. Velikov, O. D. Velev, *Curr. Opin. Colloid Interface Sci.* **2014**, *19*, 490.
- [28] a) A. Stocco, W. Drenckhan, E. Rio, D. Langevin, B. P. Binks, *Soft Matter* **2009**, *5*, 2215; b) K. Du, E. Glogowski, T. Emrick, T. P. Russell, A. D. Dinsmore, *Langmuir* **2010**, *26*, 12518; c) V. Garbin, *Phys. Today* **2013**, *66*, 68.
- [29] a) L. Isa, E. Amstad, K. Schwenke, E. Del Gado, P. Ilg, M. Kröger, E. Reimhult, *Soft Matter* **2011**, *7*, 7663; b) L. M. Foster, A. J. Worthen, E. L. Foster, J. N. Dong, C. M. Roach, A. E. Metaxas, C. D. Hardy, E. S. Larsen, J. A. Bollinger, T. M. Truskett, C. W. Bielawski, K. P. Johnston, *Langmuir* **2014**, *30*, 10188; c) A. Nelson, D. Wang, K. Koynov, L. Isa, *Soft Matter* **2015**, *11*, 118.
- [30] a) A. Graciaa, G. Morel, P. Saulner, J. Lachaise, R. S. Schechter, *J. Colloid Interface Sci.* **1995**, *172*, 131; b) K. G. Marinova, R. G. Alargova, N. D. Denkov, O. D. Velev, D. N. Petsev, I. B. Ivanov, R. P. Borwankar, *Langmuir* **1996**, *12*, 2045; c) J. Stachurski, M. Michalek, *J. Colloid Interface Sci.* **1996**, *184*, 433; d) C. Yang, T. Dabros, D. Q. Li, J. Czarnecki, J. H. Masliyah, *J. Colloid Interface Sci.* **2001**, *243*, 128; e) A. M. Elmallidy, M. Mirnezami, J. A. Finch, *Int. J. Miner. Process.* **2008**, *89*, 40; f) C. Oliveira, J. Rubio, *Int. J. Miner. Process.* **2011**, *98*, 118; g) W. H. Jia, S. L. Ren, B. Hu, *Int. J. Electrochem. Sci.* **2013**, *8*, 5828.
- [31] H. Z. Wang, V. Singh, S. H. Behrens, *J. Phys. Chem. Lett.* **2012**, *3*, 2986.
- [32] O. J. Cayre, V. N. Paunov, *Langmuir* **2004**, *20*, 9594.
- [33] A. J. Worthen, H. G. Bagaria, Y. S. Chen, S. L. Bryant, C. Huh, K. P. Johnston, *J. Colloid Interface Sci.* **2013**, *391*, 142.
- [34] R. H. Tarek, *Master Degree Thesis*, The University of Texas at Austin, December, **2012**.
- [35] M. J. Rosen, J. T. Kunjappu, *Surfactants and Interfacial Phenomena*, Wiley-VCH, Weinheim, Germany **2012**.
- [36] a) S. Crossley, J. Faria, M. Shen, D. E. Resasco, *Science* **2010**, *327*, 68; b) Z. P. Wang, M. C. M. van Oers, F. P. J. T. Rutjes, J. C. M. van Hest, *Angew. Chem. Int. Ed.* **2012**, *51*, 10746.
- [37] E. Dickinson, *Curr. Opin. Colloid Interface Sci.* **2010**, *15*, 40.
- [38] J. Frelichowska, M. A. Bolzinger, Y. Chevalier, *Colloids Surf., A* **2009**, *343*, 70.

Received: March 9, 2016
Published online: May 11, 2016